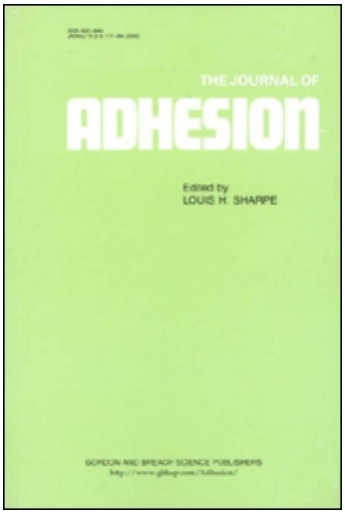

The Journal of Adhesion

Publication details, including instructions for authors and subscription information:
http://www.informaworld.com/smpp/title~content=t713453635

A Backface Strain Technique for Detecting Fatigue Crack Initiation in Adhesive Joints

Zhehua Zhang[a]; J. K. Shang[a]; F. V. Lawrence Jr.[b]
[a] Department of Materials Science and Engineering, [b] Department of Civil Engineering, University of Illinois at Urbana-Champaign, Urbana, IL, USA

To cite this Article Zhang, Zhehua , Shang, J. K. and Lawrence Jr., F. V.(1995) 'A Backface Strain Technique for Detecting Fatigue Crack Initiation in Adhesive Joints', The Journal of Adhesion, 49: 1, 23 — 36
To link to this Article: DOI: 10.1080/00218469508009975
URL: http://dx.doi.org/10.1080/00218469508009975

J. Adhesion, 1995, Vol. 49, pp. 23–36
Reprints available directly from the publisher
Photocopying permitted by license only

A Backface Strain Technique for Detecting Fatigue Crack Initiation in Adhesive Joints

ZHEHUA ZHANG, J. K. SHANG*

Department of Materials Science and Engineering

F. V. LAWRENCE, JR.

Department of Civil Engineering, University of Illinois at Urbana-Champaign, Urbana, IL 61801, USA

(Received June 25, 1994; in final form October 12, 1994)

A new backface strain technique was developed to detect fatigue crack initiation in adhesive-bonded lap joints. The technique was based on the special strain distribution in single lap joints and detected the fatigue crack initiation by the switch in the direction of the strain variation. Use of this technique not only permits the determination of fatigue crack initiation life in the joint, but also allows the site of crack initiation to be located. With the assistance of this new backface strain technique, a fatigue crack was found to initiate in the adhesive but to propagate towards the interface to continue its growth on the interface and to cause the final separation of the joint along the interface. Measurements of fatigue crack initiation lives at different stress levels indicate that the adhesive-controlled crack initiation took an increasingly greater proportion of the total fatigue life as the stress decreased, so that the lifetime in the long-life regime was dominated by the resistance of the adhesive to fatigue crack initiation.

KEY WORDS: lap joint; backface strain; finite element method; crack initiation life; SEM

1. INTRODUCTION

Joining of the same and dissimilar materials by adhesives has become increasingly widespread because of new manufacturing possibilities brought by the flexibility of adhesive bonded joints. Early use of adhesives was mostly limited to the secondary structures which experience very low stresses. With the availability of superior structural adhesives, adhesive-bonded joints are being considered for a number of load-bearing structures.[1–5] As adhesive-bonded joints move from the secondary structure to the primary load-bearing component, the mechanical performance of the joint, especially the fatigue performance, becomes a major concern.

Because of its simple geometry and good representation of real structures, the single lap joint has been widely used to assess the mechanical behavior of adhesive joints. Fatigue studies using lap joints have shown that the fatigue resistance of the adhesively-bonded joints can be comparable, or superior, to that of spot-welded structures, but it depends strongly on many variables, including joint geometry, adhesive/adherend

* Corresponding author.

combination, surface condition or pre-treatment, loading condition and environment.[5-12] Attempts to undetstand the fatigue failure processes in the joint have been largely limited to the post-failure examination of the fracture surfaces *after* the joint is broken, which often fails to yield sufficient information on the complicated processes leading to the final fracture. The only method sensing the damage processes in the joint *during* fatigue is the technique that detects the stiffness loss of the specimen as related to the initiation and propagation of fatigue cracks.[5,13] However, the detection of fatigue crack initiation using this technique is difficult because the overall stiffness is not sensitive to localized damage such as the initiation of a fatigue crack.

In this study, a backface strain technique to detect fatigue crack initiation in a single lap joint is developed. Not only can the technique be used to determine the point of fatigue crack initiation temporally *during* fatigue, but it also permits spatial determination of the location of fatigue crack initiation when coupled with cross-sectional microscopy examination of the joint. In the following, the concept of the backface strain technique is first explained and simulated by finite element analysis. This is then followed by experimental demonstration in an epoxy/steel system. The implication of the new findings based on the new technique will be discussed.

2. BACKFACE STRAIN TECHNIQUE

Consider a single lap joint, subject to a pair of parallel loads, P in Figure 1a. Because of the asymmetry of the loads, a moment develops, which casues the joint to rotate as

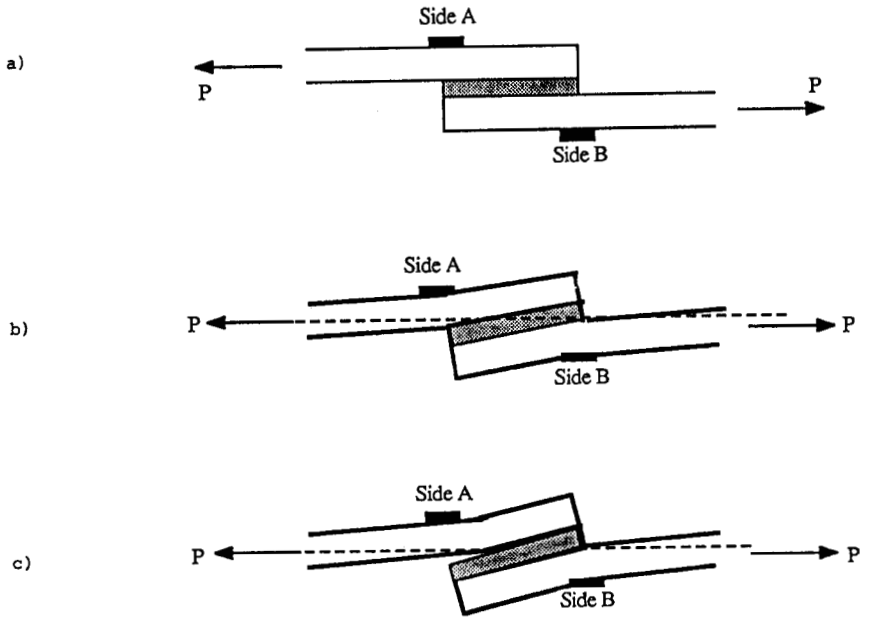

FIGURE 1 Schematic illustration of the backface strain technique: a) initial loading of a lap joint, b) joint rotation, and c) deformation of the joint after crack initiation.

shown in Figure 1b. The joint rotation produces a bending deformation in the adjoining beams. The deformation of the beam is the most severe at the ends of the overlap,[14] where two strain gauges, A and B, are placed on the "backface" of the beam (Fig. 1). When a crack appears at one of the ends (Fig. 1c), *e.g.*, point A, it relaxes the deformation of the beam locally, moving the location of the maximum strain to a point close to the crack tip. Consequently, the strain reading at the strain gauge A decreases as soon as the crack is initiated. The essence of the backface strain technique is that the downfall of the backface strain from either gauge A or B could be used as an indicator for fatigue crack initiation during fatigue loading.

To substantiate the proposed concept above, a finite element method (FEM) was used to calculate the deformation in a single lap joint made of a toughened epoxy and steel, with dimensions given in Figure 2. The same joint was used in our experimental studies to be described later. The FEM model of the specimen is shown in Figure 3. The boundary condition adopted is given in Figure 3a. The finite element mesh, produced by PATRAN (PDA Engineering, Costa Mesa, CA), are all eight-point equal-parameter elements as shown in Figure 3b. The mesh divided the specimen into 7 layers of elements in the y direction, three layers for each adherend and 1 layer for the adhesive layer. To address the stress concentration at the corners, a more refined mesh shown in Figure 3c was used. The total number of elements was 962 and nodes, 3441. Because the deformation of the adherend is elastic and our primary interest was the backface strain in the adherend, the plastic deformation in the adhesive near the region of stress concentration was neglected. All elements were linear elastic and a plane strain condition was assumed. The properties of adhesive and adherend are listed in Table I.

FEM calculations were performed using ABAQUS (Hibbitt, Karlsson & Sorensen, Pantucket, RI) at a tensile load of 2.5 kN, which produces an apparent shear stress of 3.875 MPa in the adhesive. Figure 4 shows the varition of the backface strain from one end of the overlap to the other for one of the adjoining beams. Since the backface strain is always compressive at strain gauges A and B, the sign of the backface strain throughout this paper is reversed to make compressive strain a positive value. As expected, the backface strain at the end of the beam is zero (point E). It is tensile over most of the overlap, goes through an inflection point, D, which is 10 mm from the mid-point of the overlap, changes its sign to turn compressive, reaches the maximum at the opposite end of the overlap, A or B, and gradually returns to the average strain in the beam at a distance far from the overlap.

The maximum strain at the end, A or B, depends on the stiffiness of the joint, which is determined by the elastic properties of adhesive and adherend. The effect of the

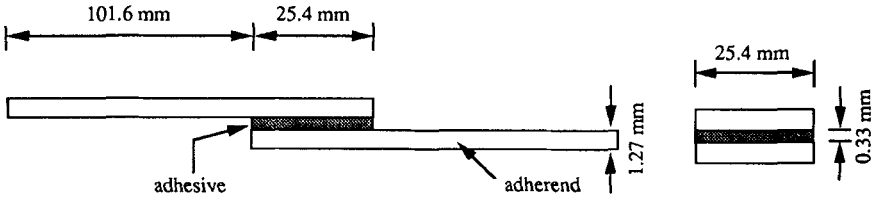

FIGURE 2 Dimensions of the lap joint studied.

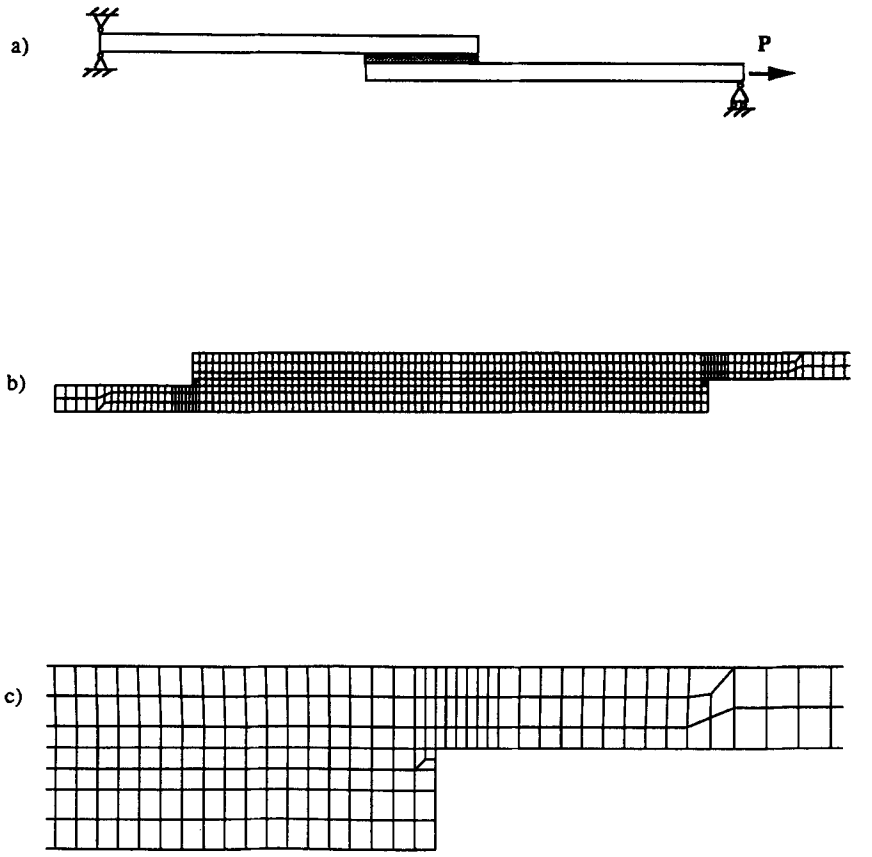

FIGURE 3 FEM model of the lap joint. Shown are a) boundary conditions used, b) FEM meshes, and c) mesh structure near the corners.

TABLE I
Room Temperature Elastic Properties of Adhesive and Adherend

Component	Material	Modulus (GPA)	Poisson's Ratio
Adhesive	Epoxy	2.25	0.4
Adherend	Steel	210	0.3

adhesive property is shown in Figure 5. When the elastic modulus of the adhesive is reduced from 5 GPa to 0.5 GPa, say, by cyclic creep polymer, the backface strain reading is increased by ~ 20 micro-strain, which can be measured by strain gauges. Therefore, the backface strain can be used to gauge the potential softening of the adhesive during fatigue loading.

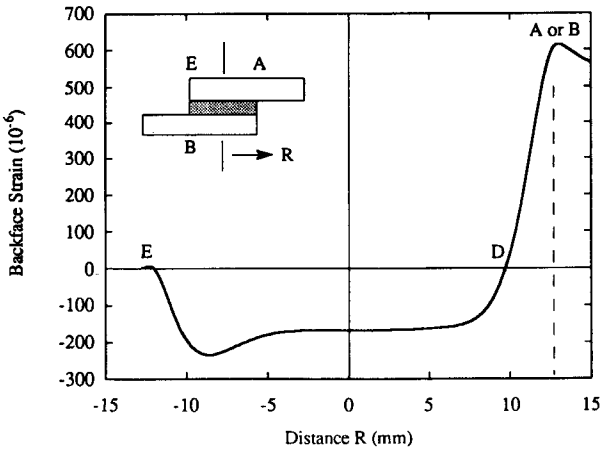

FIGURE 4 Variation of the backface strain from one end of the overlap to the other. The distance R is measured from the middle of the overlap.

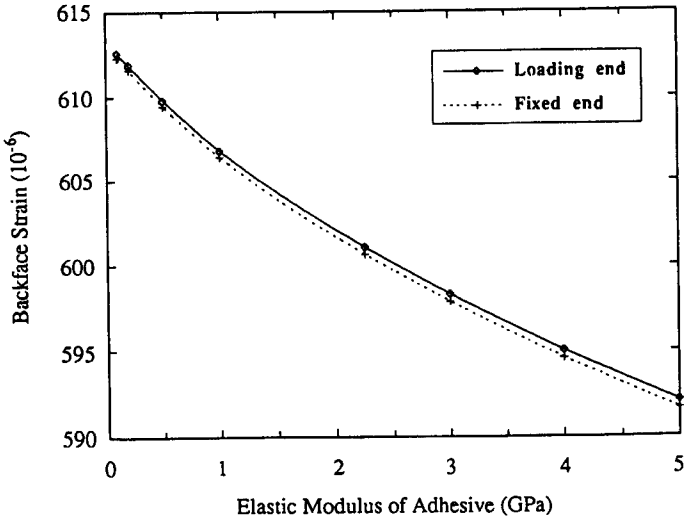

FIGURE 5 Increase of the backface strain at the end of the overlap caused by the reduction in the modulus of the adhesive.

When a crack develops at one of the ends, A, the position of the maximum strain will move with the crack tip. To simulate the crack, a cut-out was made at one end of the overlap A, along the interface between adhesive and adherend. The FEM calculation was subsequently carried out on the "cracked" joint, whose deformation is delineated in Figure 6. Compared with the deformation in the uncracked specimen (Fig. 6a), a non-symmetrical strain-distribution develops in the cracked lap joint. The strain

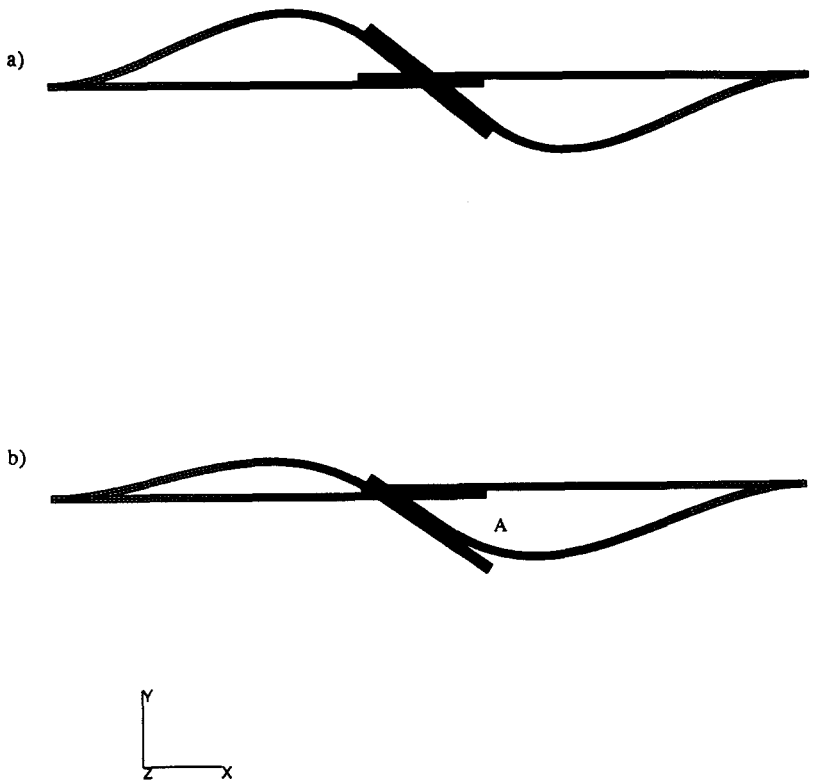

FIGURE 6 Comparison of the deformation of a) uncracked and b) "cracked" lap joints.

distribution on the backface of the upper adherend is given in Figure 7a for different crack lengths. As crack length increases, the peak in the backface strain moves ahead with the crack tip. At the same time, the peak value also increases. However, at one end of the overlap, A, the backface strain increases slightly at the beginning and then decreases rapidly with crack length (Fig. 7b). At the other end of the overlap, B, backface strain increases steadily with crack length.

For the strain gauge A, if the strain reading initially remains constant or increases with fatigue cycling because of cyclic softening of the adhesive as simulated in Figure 5, a switch of the strain variation from the increasing trend to the decreasing will indicate the appearance of a fatigue crack. The feasibility of using the turning point as an indicator of fatigue crack initiation is illustrated by the experimental studies below.

3. EXPERIMENTAL PROCEDURE

The adhesive used in this study was a toughened epoxy produced by 3M (3M designation, DP-420). The room temperature mechanical properties were measured using rectangular tensile specimens as suggested by ASTM D638. The tensile tests were

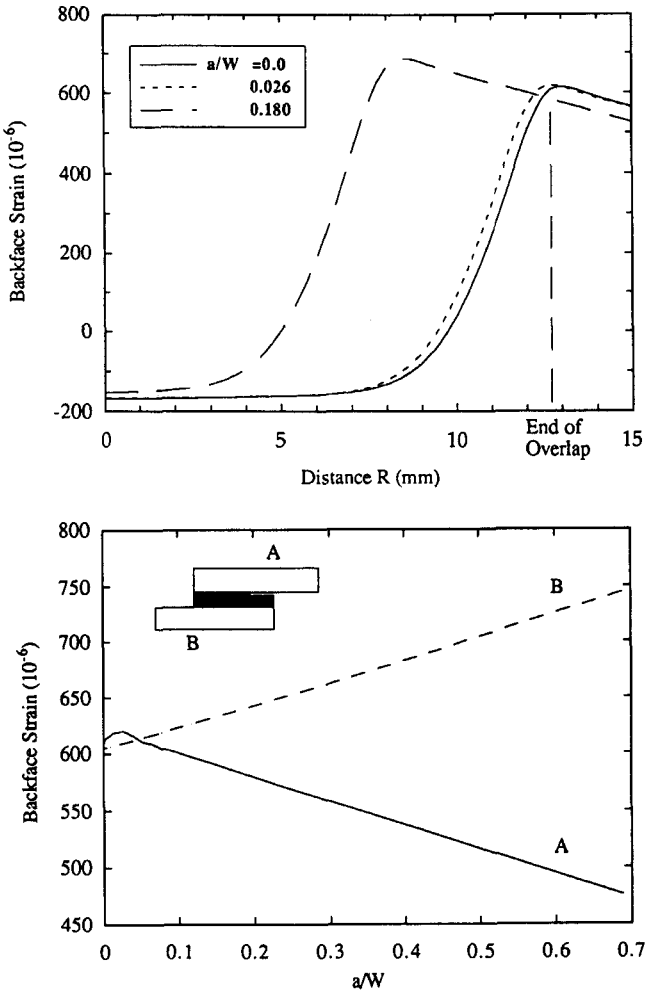

FIGURE 7 Variation of backface strain (calculated) with crack length. Shown are a) the peak movement and b) the strain at two ends of the overlap, as a function of crack length normalized by the overlap width, w.

conducted on an Instron servohydraulic machine at a crosshead speed of 0.08 mm/sec while the deformation was measured by extensometer and strain gauge rosette. The elastic properties obtained are given in Table I.

The adhesive was used to bond sheets of galvanized steel with a thickness, t_s, of 1.27 mm. The adherends were first abraded by 400 grit sand-paper and then MEK (Methyl Ethyl Ketone) rinsed before joining. The glue-line thickness was controlled by placing a few glass beads of 0.33 mm diameter at the middle of the overlap, as shown in Figure 8, after applying the adhesive. The glass beads have no effect on fatigue crack initiation because the crack always starts at the end of the joint where stress concentration exists.[15-20] The specimen was then joined by applying pressure with clips. At the

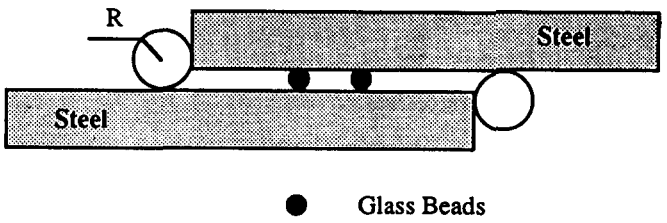

FIGURE 8 Schematic showing the control of adhesive thickness and fillet radius in specimen preparation.

ends of the overlap, fillets with a radius of 0.66 mm were introduced by pressing a cylindrical surface against the adhesive at both ends of the joint before curing (Fig. 8). The procedure has proved very effective in reducing scatter in the test data (lap shear strengths within 5%). The specimens were finally cured at room temperature for at least 7 days before being tested.

Monotonic tensile testing of the lap shear specimens were conducted at a constant strain rate of 0.01/s as per ASTM D 1002-72. Specimens were tested to failure and the strength was determined by maximum load divided by the total adhesive area. The load-displacement curve was recorded for each test to assist in the strength evaluation. The nominal/apparent shear strength of the joint was 18.9 ± 0.5 MPa.

Fatigue testing of single lap joints was carried out under load control on an MTS servohydraulic machine using a sinusoidal waveform at a load ratio, $R = 0$ (minimum load/maximum load), and a frequency of 10 Hz. The gripping arrangement is shown in Figure 9. Tests were conducted at select stress levels under constant load-amplitude in controlled laboratory air (22°C, 50%RH). To detect the fatigue crack initiation, two strain gauges were attached to the specimen according to the backface strain technique described above. The cyclic strains produced by the fatigue loading were monitored by a DAS-16 Keithley (Keithley Metrabyte, Taunton, MA) data acqusition board connected to a personal computer. The maximum value of the cyclic strain, thereafter used as the backface strain, was plotted as a function of fatigue cycle and displayed during and after experiments. Specimens were tested to the complete separation into two pieces to obtain total fatigue life. On select specimens, tests were interrupted when a peak in the backface strain began to develop. The specimen was then coated with aluminum (to enhance the contrast) and examined in a scanning electron microscope (SEM) to locate the fatigue crack.

4. EXPERIMENTAL RESULTS

The results of backface strain measurements on a lap shear joint are shown in Figure 10. The specimen had broken from the end where the strain gauge A was attacted. For the first 100,000 cycles, the backface strain remained fairly constant. Beyond 10^5 cycles, the backface strain first increased gradually and then decreased rapidly, while the backface strain at the other end B increased steadily until the fracture of the specimen. As discussed above, the turning point where the backface strain begins to fall signals the initiation of a fatigue crack at the end A.

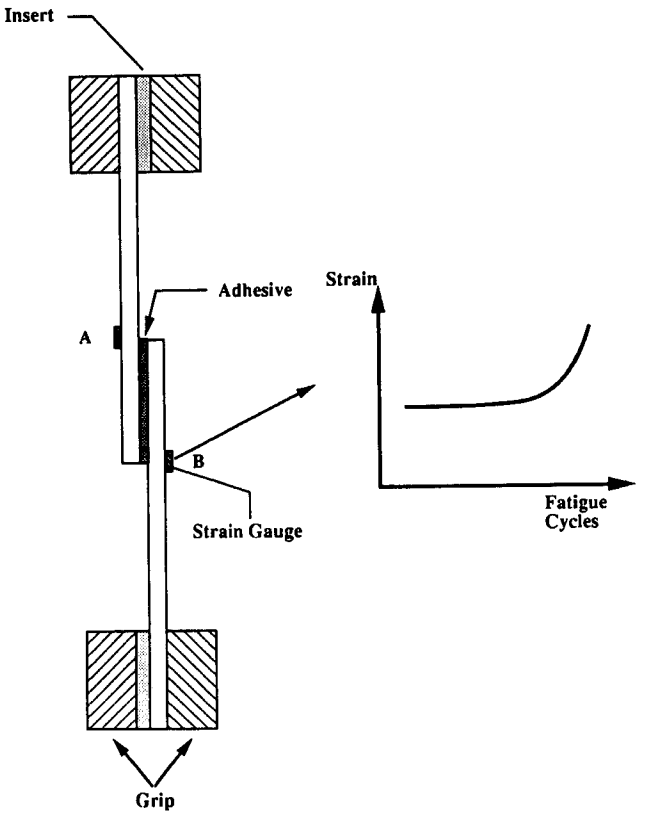

FIGURE 9 Experimental set-up for fatigue testing of lap joints. Also included are the locations of the strain gauges to monitor the backface strain.

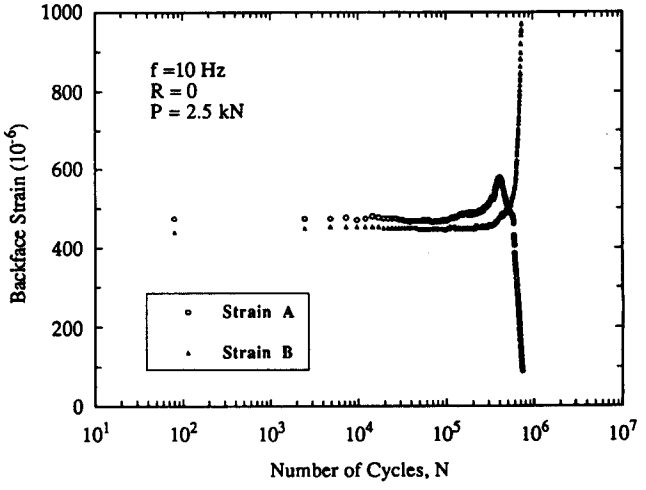

FIGURE 10 Backface strain readings from the two strain gauges mounted on the specimen shown in Figure 9.

The confirm this, the test was repeated on a second specimen, but the fatigue loading was interrupted when a peak in the backface strain began to develop or right after the downfall in the backface strain began. The fatigued specimen was then removed from the testing machine and examined in the SEM. Fatigue cracks were indeed found at the end A, as shown in Figure 11. Multiple cracks had initiated in the polymer adhesive near the fillet. One crack extended from the surface of the fillet to the interface, and had propagated along the interface. Continued testing led to the complete failure of the specimen along the interface.

The detection of very small cracks during the fatigue loading by the backface strain technique means that the turning point or the peak in the backface strain reading can be used to define the point of fatigue crack initiation. This definition divides the total fatigue life, N_f, into the portion prior to the initiation when the fatigue damage is accumulated, or the initiation life, N_i, and the portion after, which is spent to propagate the fatigue crack, or the propagation life, N_p. The fatigue crack propagation is a separate subject and will not be treated here. As shown in Figure 12, the initiation life strongly depends on the applied stress, similar to the stress-life (N_f) relationship. However, the lines in Figure 12 are not parallel, indicating that the factors influencing N_i and N_f may not be same at different stress levels or in different regimes of lifetimes.

An analysis of the role of fatigue crack initiation is given in Figure 13. At low cycles, fatigue crack initiation is relatively easier so that most of the lifetime is spent in propagating the crack; N_i is a poor representation of N_f. However, as one requires a long fatigue life or moves to the high cycle regime, the role of fatigue crack initiation

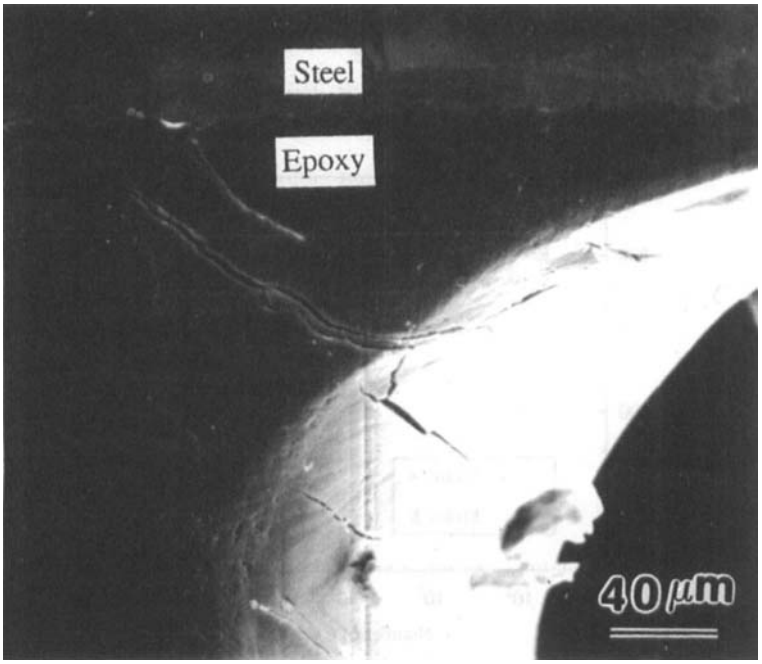

FIGURE 11 Fatigue cracks in the joint when the peak in the backface strain began to develop.

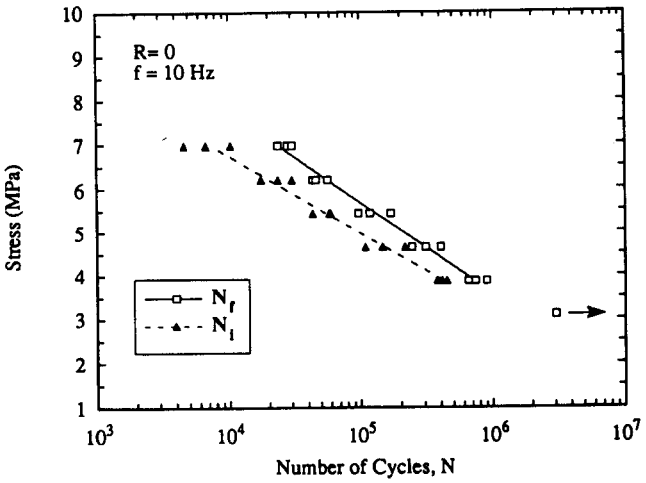

FIGURE 12 Fatigue cycles required to initiate fatigue cracks, N_i, or to break the lap shear specimens, N_f, at different applied stresses.

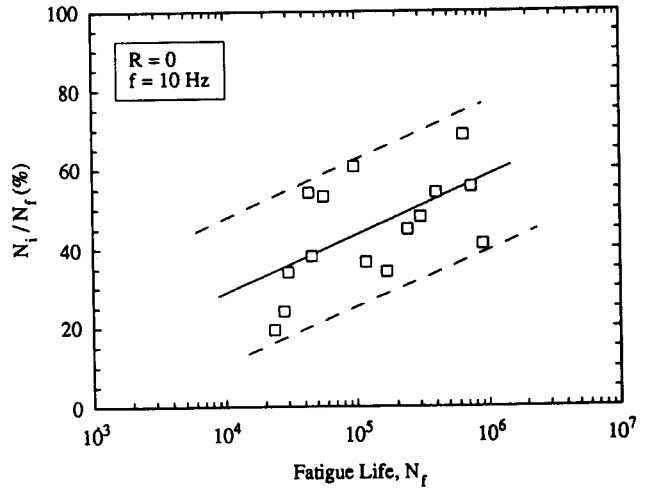

FIGURE 13 Ratios of the fatigue crack initiation over the total fatigue life at different lifetimes.

becomes inceasingly more important. If the upward trend in Figure 13 could be trusted to continue, at the lifetime of 10^7, which is often used to define the fatigue limit in metals, a majority of the lifetime would be devoted to initiating the fatigue crack.

5. DISCUSSION

The theoretical analysis and experimental results have shown that the backface strain technique is a viable method to detect the initiation of fatigue cracks in a lap joint. The

implementation of the technique requires attaching two strain gauges at two ends of the overlap. In theory, the fatigue crack initiation coincides with the peak in the backface strain at the end of the overlap. However, the actual position of the peak in the backface strain may be shifted because of the finite gauge length and the precise location of the strain gauge.

Because of its finite gauge length, the strain gauge samples, and takes the average of, the strain over a distance equal to the gauge length of the wires in the gauge. The implication of this averaging to the position of the peak in the backface strain was modelled by the FEM analysis and the results are presented in Figure 14. As the gauge length increases, the peak in the backface strain reading is delayed to longer and longer crack lengths or moved to a point further and further away from the exact end point of the overlap. For long gauge lengths, the backface strain peaks when the crack length is about the half length of the gauge. Therefore, for better sensitivity, a smaller gauge is preferred.

The relative movement in the peak position of the backface strain with respect to the end of the overlap suggests that an adjustment may be made in the location of the strain gauge to offset the shift in the peak position away from the end of the overlap. In the FEM analysis, the adjustment was made by moving the center of the strain gauge, relative to the end of the overlap, by an offset distance, d, as shown in Figure 15a. The resulting changes in the backface strain are given in Figure 15b for different offsets at the fixed gauge length of 4 mm. Again, at the zero offset, the peak of the backface strain is attained at 2 mm from the end of the overlap. With an offset distance of 2.0 mm, the initial increase of the backface strain with crack length essentially disappears so that the decrease in the backface strain coincides with the initiation of a very small crack.

The implications of Figure 15 are as follows. On the one hand, the strong dependence of the peak position on the offset distance requires consistency in placing the strain gauges so that the measurements of N_i may be compared. On the other hand, with the

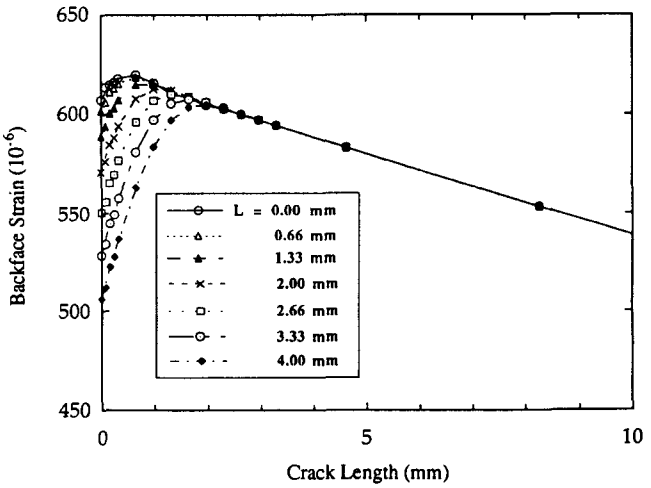

FIGURE 14 Variation of the backface strain with crack length at different gauge lengths.

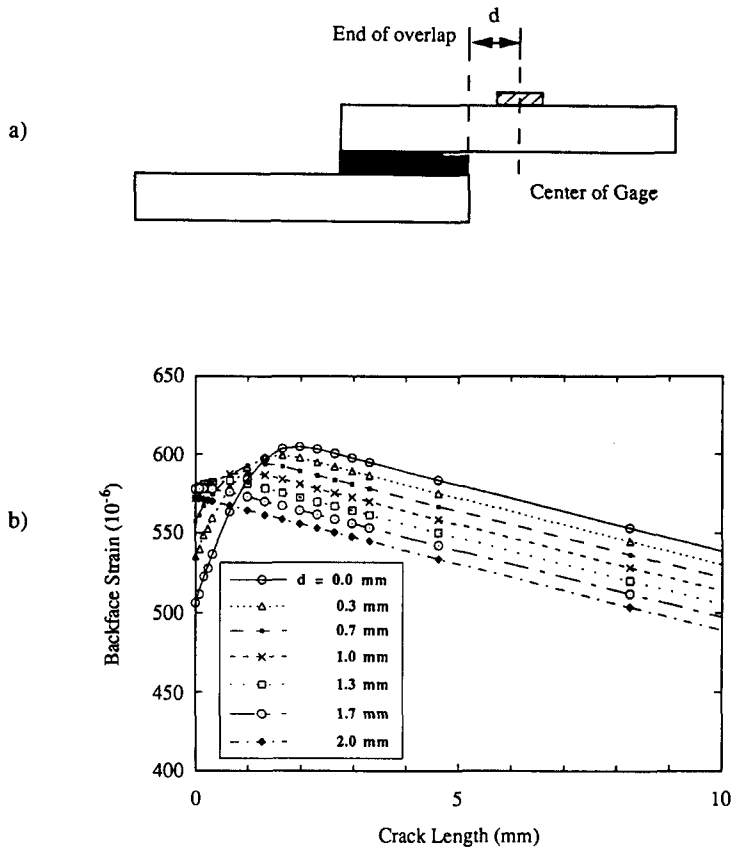

FIGURE 15 Dependence of the backface strain on the precise location of the strain gauge: a) strain gauge placed at an offset distance, *d*, away from the end of the overlap, and b) calculated backface strain from the strain gauge in a).

knowledge in Figure 15, one could tune the sensitivity of the backface strain technique in detecting fatigue cracks by specifying an optimum offset distance so that cracks may be caught early when they are still very small. Moreover, presumably, one should be able to detect the length of the fatigue crack by scanning the backface strain at different offset distances and determining the crack length from the peaks of the backface strain.

While the decay in the backface strain can be related to the formation and propagation of a fatigue crack if a proper offset distance is chosen for a finite strain gauge length, the physical basis for the variation of the backface strain prior to the fatigue crack initiation is not certain. Early FEM simulation demonstrated that the increase in the backface strain could arise from cyclic softening of the adhesive, but other processes such as localized plastic deformation of the adhesive near the end fillets may also contribute. Further studies are clearly needed to understand better the mechanism for strain accumulation so that a criterion for fatigue crack initiation may be established. By detecting the point of the fatigue crack initiation, the backface strain technique can serve as a useful tool in search of an appropriate criterion.

6. CONCLUSIONS

Based on our investigation of the deformation and failure processes in a lap joint, the following conclusions have been rached:

1. The backface strain reading at the end of the overlap can serve as an indicator of the fatigue crack initiation in the joint. Fatigue crack initiation can be detected by the switch in the direction of the backface strain variations with fatigue cycle.
2. The ability of the backface strain technique to detect a fatigue crack depends on the gauge length of the strain measurement device and on relative position of the strain gauge with respect to the end of the overlap.
3. In an epoxy/steel joint, fatigue cracks were found to initiate in the adhesive at the end fillet of the lap joint. The fatigue crack propagated from the adhesive to the interface and continued to propagate along the interface to cause the final fracture of the specimen.
4. Both total life and fatigue crack initiation life decreased with applied stress, but the dependence of the fatigue crack initiation life on applied stress was different from the dependence of the total life on stress. Fatigue crack initiation was more important in the high cycle regime.

Acknowledgment

Support was provided by the Ford Motor Company and the Fracture Control Program at the University of Illinois. Special thanks are due to Drs. G. Banas and P. Kurath for experimental assistance.

References

1. W. J. Renton and J. R. Vinson, *J. Adhesion* **7**, 175 (1975).
2. M. Imanaka, Y. Fukuchi, W. Kishimoto, K. Okita, H. Nakayama and H. Nakai, *ASME J. Engng. Mater. Tech.* **110**, 350 (1988).
3. M. Imanaka, K. Haraga and T. Nishikawa, in "Composite Matls. Tech. 1990", *Proc. 13th Annual Energy Source Tech. Conference and Exhibition*, 1990, pp 89–93.
4. Chiaki Sato and Kozo Ikegami, *J. Adhesion* **39**, 29 (1992).
5. J. A. Harris and P. A. Fay, *Int. J. Adhesion and Adhesives* **12**, 9 (1992).
6. R. A. Chernenkoff, *SMAPE* **21**, 57 (1989).
7. C. Ciezskiewicz, G. Banas, and F. V. Lawrence, Report to the Americal Iron and Steel Institute, December 1991.
8. A. J. Kinloch, *J. Mater. Sci.* **17**, 617 (1982).
9. P. D. Mangalgiri, W. S. Johnson and R. A. Everett, *J. Adhesion* **23**, 263 (1987).
10. S. Mostovoy, P. B. Crosely and E. J. Ripling, *Adhesion Sci. Tech.* **9B**, L. H. Lee, Ed. (Plenum Press, New York, 1975), p. 513.
11. S. S. Wang and J. F. Yau, *Int. J. Fracture* **19**, 295 (1982).
12. S. Mall and G. R. Ramamurthy, *Int. J. Adhesion and Adhesives* **9**, 33 (1989).
13. Makoto Imanaka *et al.*, in *Fatigue Mechnisms of Adhesive Bonded Joint*, Published by Int. Assoc, for Structural Safety and Reliability, pp. 713–718, 1985.
14. J. L. Hart-Smith, *ASTM STP* **876**, 238 (1985).
15. G. R. Wooley and D. R. Carver, *J. Aircraft* **8**, 817 (1971).
16. D. J. Allman, *J. Mech. Appl. Math* **30**, 415 (1977).
17. F. Delale and F. Erdogan, *J. Appl. Mech* **48**, 331 (1981).
18. J. A. Harris and R. D. Adams, *Int. J. Adhesion and Adhesives* **4**, 65 (1984).
19. W. C. Carpenter, *J. Adhesion* **35**, 55 (1991).
20. R. D. Adams and V. Mallick, *J. Adhesion* **38**, 199 (1992).